Related commentary on page 805

The American Journal of Pathology, Vol. 170, No. 3, March 2007

DOI: 10.2353/ajpath.2007.060960

Vascular Biology, Atherosclerosis and Endothelium Biology

Endothelial-Specific Expression of Mitochondrial Thioredoxin Improves Endothelial Cell Function and Reduces Atherosclerotic Lesions

Haifeng Zhang,* Yan Luo,*† Wei Zhang,*‡ Yun He,* Shengchuan Dai,* Rong Zhang,* Yan Huang,* Pascal Bernatchez,* Frank J. Giordano,* Gerald Shadel,§ William C. Sessa,* and Wang Min*§

From the Interdepartmental Program in Vascular Biology and Transplantation, Boyer Center for Molecular Medicine, and Department of Pathology,§ Yale University School of Medicine, New Haven, Connecticut; the State Key Laboratory of Ophthalmology,† Zhongshan Ophthalmic Center, Sun Yat-Sen University, Guangzhou, China; and the Key Laboratory of Combined Multi-Organ Transplantation of Ministry of Health China,‡ The First Affiliated Hospital, Zhejiang University College of Medicine, Hangzhou, China*

The function of the mitochondrial antioxidant system thioredoxin (Trx2) in vasculature is not understood. By using endothelial cell (EC)-specific transgenesis of the mitochondrial form of the thioredoxin gene in mice (Trx2 TG), we show the critical roles of Trx2 in regulating endothelium functions. Trx2 TG mice have increased total antioxidants, reduced oxidative stress, and increased nitric oxide (NO) levels in serum compared with their control littermates. Consistently, aortas from Trx2 TG mice show reduced vasoconstriction and enhanced vasodilation. By using ECs isolated from Trx2 TG mice, we further show that Trx2 increases the capacities of ECs in scavenging reactive oxygen species generated from mitochondria, resulting in increases in NO bioavailability in ECs. More importantly, Trx2 improves EC function and reduces atherosclerotic lesions in the apolipoprotein E-deficient mouse model. Our data provide the first evidence that Trx2 plays a critical role in preserving vascular EC function and prevention of atherosclerosis development, in part by reducing oxidative stress and increasing NO bioavailability. ***(Am J Pathol 2007, 170:1108–1120; DOI: 10.2353/ajpath.2007.060960)***

It has become clear that increases in reactive oxygen species (ROS; ie, H_2O_2, O_2^-, and ·OH) and inflammatory mediators [such as tumor necrosis factor (TNF)] represent a common pathogenic mechanism for atherosclerosis.[1–4] The vascular cell that normally limits the inflammatory and atherosclerotic process is the endothelial cell (EC). ROS and TNF induce EC dysfunction that is characterized by a reduction in amount of bioavailable nitric oxide (NO) in the vasculature and an enhanced sensitivity of vascular cells to proapoptotic stimuli. NO serves to regulate vasomotion[5] and to suppress atherosclerosis by reducing EC activation, smooth muscle cell proliferation, leukocyte-EC interaction, and platelet aggregation and adhesion.[6,7] Because NO can be inactivated by ROS, it is postulated that ROS-induced reduction in NO bioavailability promotes the proatherogenic state of the vessel wall.

ROS-producing systems are numerous and include various NAD(P)H oxidases, xanthine oxidase, and the uncoupling of NO synthase as well as mitochondria.[1–4] The NAD(P)H oxidases have been considered predominant sources of ROS in the pathogenesis of hypertension, atherosclerosis, cardiac hypertrophy, and heart failure.[4,8] However, recent data suggest that mitochondrial proteins are especially vulnerable to oxidation in response to stress stimuli including proinflammatory cytokines.[9] Furthermore, there is increasing evidence supporting that ROS generated from mitochondria significantly contributes to EC dysfunction and the progression of atherosclerosis.[1,2,10,11] A recent report demonstrated that overexpression of catalase in mitochondria, but not in other cellular compartments, extended the life span of mice.[10] Mitochondrial electron transport

Supported by the National Institutes of Health (grants R01 HL-65978-5 and P01HL070295-6 to W.M.). W.M. is an established investigator of the American Heart Association (0440172N).

H.Z., Y.L., W.Z., and Y.H. contributed equally to this work.

Accepted for publication November 29, 2006.

Supplemental material for this article can be found on *http://ajp.amjpathol.org.*

Address reprint requests to Dr. Wang Min, Interdepartmental Program in Vascular Biology and Transplantation, Department of Pathology, Yale University School of Medicine, BCMM 454, 295 Congress Ave., New Haven, CT 06510. E-mail: wang.min@yale.edu.

chains consume oxygen by oxidative phosphorylation to form ATP. During this process, between 0.4 to 4% of the consumed oxygen is released in the mitochondria as ROS resulting from the univalent reduction of molecular oxygen to O_2^- by electrons that leak from complex I and III of the mitochondrial electron transport chain. O_2^- is in turn converted to H_2O_2 by mitochondria-specific manganese-dependent superoxide dismutase (MnSOD). H_2O_2 is itself a mild oxidant and is readily converted to the powerful oxidant ·OH via the Fenton reaction. These ROS (O_2^-, H_2O_2, and ·OH) can cause multiple cellular actions if they are not appropriately regulated.[12] In ECs, O_2^- not only alters endothelium-dependent vascular relaxation through interaction with NO, but the resultant formation of peroxynitrite can also oxidize the essential eNOS cofactor tetrahydrobiopterin (BH_4), which may promote endothelial nitric-oxide synthase (eNOS) uncoupling.[13] However, the role of H_2O_2 in the regulation of NO bioactivity *in vivo* is unclear. It has been shown that on binding to a peroxidase such as catalase, H_2O_2 forms compound I, which oxidizes NO to nitrogen dioxide anion (nitrite, NO_2^-) and reacts with NO_2^- to form nitrogen dioxide radical ($NO_2^{\cdot}$). $NO_2^{\cdot}$ in turn participates in nitrating events such as the formation of nitrotyrosines in proteins.[14] It has also been reported that eNOS is regulated by H_2O_2 (but not O_2^-) posttranscriptionally and posttranslationally.[15] In addition, ROS (particularly H_2O_2) may function as a second messenger in signal transduction and regulate EC growth/proliferation, apoptosis, EC barrier function, vasorelaxation, and vascular remodeling.[14,16,17]

Thioredoxin (Trx) is a small, multifunctional protein that has a redox-active site (sequence Cys32-Gly-Pro-Cys35). Although Trx1 is localized in cytosol, Trx2 was identified in mitochondria.[18] Trx2 has a conserved Trx catalytic site and a consensus signal sequence for mitochondrial translocation. Trx2, like Trx1, contains the redox-active site (C90 and C93) and probably undergoes reversible oxidation to the Cys disulfide (Trx-S2) through the transfer of reducing equivalents from the catalytic site Cys residues to a disulfide protein substrate (protein-S2), thus maintaining the protein in a reduced state. The reduced form of Trx is then regenerated by Trx reductase (TrxR) at the expense of NAPDH.[19] Mitochondria have the most reducing environment among all cellular organelles, and a reduced state is critical for maintaining the mitochondria electrochemical potential, generation of ATP and eliminating ROS.[9] In addition to MnSOD defending against O_2^- in the mitochondria,[20] recent data suggest mitochondria also contain a specific Trx2, Trx2-dependent peroxidase (Prx3), and Trx2 reductase (TrxR2), providing a primary line of defense against ROS produced by the mitochondrial respiratory chain. Indeed, cells with deficiency or knockdown of Trx2 or Prx3 accumulate endogenous ROS and are highly sensitive to exogenous oxygen radicals.[20,21] However, little is known about the function and roles of the Trx2 system in vasculature.

In the present study, by using EC-specific transgenesis of Trx2, we demonstrate a critical role of Trx2 in regulating several functions of the endothelium. Specifically, isolated aortas from Trx2 TG mice show increases in NO bioavailability and enhanced endothelium-dependent vasodilation. We use ECs isolated from Trx2 TG mice to show that Trx2 increases the capacities of ECs in scavenging ROS generated by mitochondria, resulting in increases in NO bioavailability in ECs. More importantly, we demonstrate that EC expression of Trx2 improves EC function and reduces atherosclerotic lesions in an ApoE-deficient mouse model. Our data provide the first evidence that Trx2 plays a critical role in preserving vascular EC function and prevention of atherosclerosis development.

Materials and Methods

Animal Protocol

Mice were housed in specific pathogen-free animal facilities according to guidelines from the Office of Laboratory Animal Welfare at the National Institutes of Health, and all experimental procedures were approved by the institutional animal care and use committees at Yale University, New Haven CT.

Generation of the Transgene Construct pVE-Trx2

The VE-cadherin promoter in TA vector was obtained from Dr. Laura Benjamin (Harvard Medical School, Boston, MA). The 3′-UTR (untranslated region) from bovine growth hormone (bGH) was cloned into downstream of the VE-cadherin promoter to generate pVE-pA vector. The human Trx2 cDNA with an HA-tag sequence at the 3′-end was inserted into the *Eco*RI and *Xba*I sites between the VE-cadherin promoter and bGH pA to obtain pVE-Trx2 plasmid. The plasmid was linearized with *Xho*I digestion, and the pronuclear injection was performed at Yale Transgenic Core. The founder transgenics were identified by polymerase chain reaction (PCR) of tail DNA with a 5′ primer of Trx2 and 3′ primer of HA. Trx2 TG mice were backcrossed with C57BL/6 mice for more than six generations before experiments. All experiments were performed with heterozygous Trx2 TG mice and their non-TG littermates as controls.

ROS Detection by Flow Cytometry Analysis

For measurement of total intracellular ROS, we used 5,6-chloromethyl-2′,7′-dichlorodihydrofluorescein diacetate (CM-H_2DCFDA, preferentially for H_2O_2) or dihydroethidium (preferentially for superoxide). For measurement of total intracellular ROS, dihydrorhodamine 123 (DHR123, preferentially for H_2O_2), or MitoTracker Red CM-H_2XROS (MitoROS, preferentially for superoxide). All probes were purchased from Molecular Probes, Eugene, OR. Cells were loaded with 5 μmol/L of a indicated probe and were incubated at 37°C for 20 minutes and were immediately detached and subjected to analytic flow cytometry on a FACSort (BD Biosciences, San Jose, CA). The fluorescence signal was recorded on the FL1 (green) or FL3 (red) channel and analyzed by using CellQuest software. As controls, cells were treated with TNF (10

ng/ml), paraquat (1 mmol/L), or H_2O_2 (1 mmol/L) for indicated times.

Serum NOx, Total Antioxidant, and Free 8-Isoprostane Assays

NOx (both nitrite and nitrate) in serum was determined by an assay kit from Cayman Chemical, Ann Arbor, MI. Total antioxidant levels in serum was determined by the Total Antioxidant Assay kit from Calbiochem, La Jolla, CA. The assay relies on the ability of antioxidants in the sample to inhibit the oxidation of ABTS [2,2′-azino-di-(3-ethylbenzthiazoline sulfonate)] to $ABTS^+$ by metmyoglobin (a peroxidase). The amount of $ABTS^+$ produced can be monitored by reading the absorbance at 600 nm. 8-Isoprostane in serum was determined by an enzyme-linked immunosorbent assay kit from Cayman Chemical. The isoprostanes are a family of eicosanoids of nonenzymatic origin produced by random oxidation of tissue phospholipids by oxygen radicals.

NO Release, eNOS Phosphorylation, and eNOS Enzymatic Assay

NO levels in serum or EC media were assessed by measuring nitrite levels using a NO-specific chemiluminescence analyzer (Sievers, Boulder, CO). Data are reported as NO_2^- accumulation per mg of protein.[22] Serum or media were deproteinized and samples containing NO_2^- were refluxed in glacial acetic acid containing sodium iodide. Under these conditions, NO_2^- was quantitatively reduced to NO, which was quantified by a chemiluminescence detector after reaction with ozone in a NO analyzer. In all experiments, NO_2^- release was inhibitable by a NOS inhibitor. The eNOS activity assay was determined based on the conversion of [^{3}H]L-arginine to [^{3}H]L-citrulline and was performed according to the protocol provided by the manufacturer (nitric-oxide synthase assay kit; Calbiochem). Data are presented as pmol of [^{3}H]L-citrulline per minute per protein. In some experiments, cells were treated with vascular endothelial growth factor (VEGF) (10 to 50 ng/ml) for 30 minutes as a positive control for NO release, eNOS phosphorylation, and eNOS enzymatic assays.

Mouse EC Culture

Mouse aortic EC isolation from wild-type (WT) and Trx2 TG mice was performed as follows. For immunoselection, 10 μl of beads (per T-75 of mouse lung cells) were washed with 1 ml of buffer A [phosphate-buffered saline (PBS) + 2% fetal bovine serum] for three times and resuspended in 100 μl of buffer A. Ten μl (10 μg) of anti-mouse ICAM-2 or 10 μl (10 μg) of PECAM-1 were added and rocked at 4°C for 2 hours. Beads were washed for three times and resuspended in 160 μl of buffer A. Confluent mouse aortic cells cultured in a T-75 flask were placed at 4°C for 5 minutes and incubated with the beads at 4°C for 1 hour. Cells were then washed with warm PBS and treated with 3 ml of warm trypsin/ethylenediaminetetraacetic acid. When cells were detached, 7 ml of growth media were added. An empty 15-ml tube was placed in the magnetic holder, and the cell suspension (~10 ml) was added slowly by placing the pipette on the wall of the tube so that the cells pass through the magnetic field. Cells were incubated for 5 minutes, and the media were carefully aspirated. The 15-ml tube was removed from the magnetic holder, and the beads/cells were resuspended in 10 ml of media. The selected cells were plated on 0.2% gelatin-coated flasks and cultured for 3 to 7 days. When the cells were confluent, another round of immunoselection was repeated. The purity of EC population was more than 98% as determined by DiI-LDL-FITC staining followed by flow cytometry analyses.

Isolation of Mitochondria and Mitochondrial Fractions

Cultured MECs were resuspended in ice-cold RSB buffer (10 mmol/L NaCl, 1.5 mmol/L Mgcl2, and 10 mmol/L Tris-HCL, pH 7.5) to swell for 5 to 10 minutes followed by homogenization by several strokes with the B pestle. Cell lysates were added with 2.5× MS buffer (525 mmol/L mannitol, 175 mmol/L sucrose, 12.5 mmol/L Tris-HCl, pH 7.5, and 2.5 mmol/L ethylenediaminetetraacetic acid, pH 7.5) to a final concentration of 1× MS followed by centrifugation at 1300 × *g* for 5 minutes to remove nuclei, unbroken cells, and large membrane fragments. The supernatant was centrifuged at 17,000 × *g* for 15 minutes followed by 2× of wash with 1× MS buffer. The supernatant was collected as the cytoplasmic fraction. The pellet was resuspended in 1× MS buffer and followed by an ultracentrifugation at 60,000 × *g* for 20 minutes in a 30-ml gradient (15 ml of 1.0 mol/L sucrose layering over 15 ml of 1.5 mol/L sucrose in Ultraclear tubes). The mitochondria were collected from the layer at the 1 mol/L/1.5 mol/L interface with a Pasteur pipette using a gentle sweeping motion across the top of the 1.5 mol/L layer.

Immunoblotting and Antibodies

ECs (human umbilical vein endothelial cells, bovine aortic endothelial cells, or MECs) after various treatments were washed twice with cold PBS and lysed in 1.5 ml of ice-cold lysis buffer (50 mmol/L Tris-HCl, pH 7.6, 150 mmol/L NaCl, 0.1% Triton X-100, 0.75% Brij 96, 1 mmol/L sodium orthovanadate, 1 mmol/L sodium fluoride, 1 mmol/L sodium pyrophosphate, 10 μg/ml aprotinin, 10 μg/ml leupeptin, 2 mmol/L phenylmethyl sulfonyl fluoride, and 1 mmol/L ethylenediaminetetraacetic acid) for 20 minutes on ice. Protein concentrations were determined with a Bradford Protein Assay kit (Bio-Rad, Hercules, CA). The cell lysates were subjected to sodium dodecyl sulfate-polyacrylamide gel electrophoresis followed by immunoblotting (Immobilon P; Millipore, Milford, MA) with a specific antibody. The chemiluminescence was detected using an enhanced chemiluminescence kit according to the instructions of the manufacturer (Amersham Life Science, Arlington Heights, IL). Anti-cytochrome *c* antibody

was purchased from BD PharMingen (San Diego, CA), anti-catalase from Calbiochem, anti-nitrotyrosine from Chemicon (Temecula, CA), anti-V5 from Invitrogen (Carlsbad, CA), anti-Prx3 from LabFrontiers (Seoul, Korea), anti-HA from (Roche, Indianapolis, IN), anti-β-tubulin from Santa Cruz Biotechnology (Santa Cruz, CA), total and phospho-eNOS antibodies from Transduction Laboratory (Lexington, KY), and anti-TrxR2 from Upstate Technology (Lake Placid, NY). Trx1 and Trx2 were generated in our laboratory.

RNA Isolation and Quantitative Real-Time Reverse Transcriptase (RT)-PCR

Total RNA was isolated from ECs with Qiagen RNeasy mini kit (Qiagen Inc., Valencia, CA) as recommended by the supplier. Total RNA was quantitated by optical density (OD) at 260 using a Du-64 spectrophotometer (Beckman, Columbia, MD). Using equal amounts of total RNA (200 ng) from ECs, stimulated under various conditions, mRNA was primed with random hexamers, and complementary DNA (cDNA) was synthesized from mRNA by TaqMan reverse transcription with MultiScribe reverse transcriptase (PE Applied Biosystems, Foster City, CA) according to the manufacturer's description. The final cDNA product was used for subsequent cDNA amplification by polymerase chain reaction. cDNA was amplified and quantitated by using SYBR Green PCR reagents from PE Applied Biosystems according to the manufacturer's instructions. Briefly, the cDNA for the specific genes (Trx2 and 18S rRNA) were amplified by Amplitaq Gold DNA polymerase using specific primers, which were synthesized by Yale HHMI/Keck oligonucleotide synthetic facility (Yale University School of Medicine, New Haven, CT). The cDNA for 18S rRNA was amplified by using a specific forward primer (5′-TTCCGATAACGAACGAGACTCT-3′) and a specific reverse primer (5′-TGGCTGAACGCCACTTGTC-3′). The PCR reaction mixture (final volume, 25 μl) contained 5 μl of cDNA, 1 μl of 10 μmol/L forward primer, 1 μl of 10 μmol/L reverse primer, 2.5 μl of PCR 10× SYBR Green PCR buffer, 3 μl of 25 mmol/L $MgCl_2$, 2 μl of dNTP mix (2.5 mmol/L dATP, 2.5 mmol/L dCTP, 2.5 mmol/L dGTP, and 5 mmol/L dUTP), 0.25 μl of AmpErase UNG (1 U/μl uracil-*N*-glycosylase), 0.125 μl of Amplitaq Gold DNA polymerase (5 U/μl Amplitaq Gold DNA polymerase), and 10.125 μl of H_2O. The PCR reaction was performed in triplicate (three wells of a C96-well plate). The reaction was amplified with iCycler iQ multicolor real-time PCR detector (Bio-Rad) for 37 cycles with melting at 94°C for 30 seconds, an annealing at 58°C for 30 seconds, and extension at 72°C for 1 minute in iCycler iQ PCR 96-well plates (Bio-Rad). The relative quantification values for the interest gene expression were calculated from the accurate CT, which is the PCR cycle at which an increase in reporter fluorescence from SYBR Green dye can be first detected obtained above a baseline signal. CT values for 18S rRNA cDNA were subtracted from CT values for the interest gene cDNA for each well to calculate −CT. The triplicate −CT values for each sample were averaged. To calculate the fold induction of the interest gene mRNA in cells treated with cytokines over control cells, the averaged −CT values calculated for control cells was subtracted from −CT values calculated for cytokine-treated cells to calculate −CT. Then, the fold induction for each well was calculated by using 2 − (−CT) formula. The fold induction value for triplicate wells was averaged, and data are presented as the mean ± SE of triplicate wells.

Indirect Immunofluorescence Confocal Microscopy

Fixation, permeabilization, and staining of cultured ECs were performed as described previously.[23] Alexa Fluor 488 (green) or 594 (red) conjugated-secondary antibodies (Molecular Probes) were used. Confocal immunofluorescence microscopy was performed using an Olympus confocal microscope and acquired images were transferred to Photoshop 6.0 to generate the final figures (Adobe Systems, Mountain View, CA).

Immunohistochemistry for Transgene Expression

Eight- to 10-week-old Trx2 TG or WT littermates were perfused with PBS for 5 minutes and then with 4% paraformaldehyde for 5 minutes at physiological temperature and pressure. Blood vessels were then harvested and diffusion-fixed overnight at 4°C and then dehydrated in 30% sucrose overnight at 4°C. The vessels were then embedded, and 5-mm sections were stained for rat high-affinity anti-HA antibody (Roche) followed by Alexa Fluor 594 (red)-conjugated anti-rat secondary antibody. Endothelium was visualized by goat anti-CD31 antibody (Santa Cruz Biotechnology) followed by Alexa Fluor 488 (green)-conjugated anti-rat secondary antibody.

Hemodynamic and Echocardiography Studies

Anesthesia was induced by intramuscular ketamine injection. Mice were then intubated, placed on positive pressure ventilation, and light anesthesia maintained by inhaled isoflurane. The right common jugular vein was cannulated with polyethylene tubing and a 1.9 French transducer-tipped catheter (Millar Inc., Houston, TX) was advanced into the left ventricle via the right carotid artery. Left ventricular pressures, including high-fidelity positive and negative dP/dt, were measured under basal conditions and during intravenous infusion of graduated doses of dobutamine. Data were recorded by using MacLab software and were analyzed by using the Heartbeat program (University of California at San Diego, San Diego, CA). Echocardiograms were obtained on lightly anesthetized mice (isoflurane inhalation via nosecone) by using a 15-Mhz transducer and a Sonos 7500 console (CVS, Aliso Viejo, CA). Zoomed two-dimensional images were used to determine a short axis plane at the level of the papillary muscles, and then M-mode was obtained at this level. Measurements were obtained using the 7500 analysis software.

Aortic Ring Assay

The thoracic aorta is dissected from both male and female mice (8 to 10 weeks of age) and cut into cylindrical, 3-mm-long segments. The rings are suspended by two tungsten wires mounted in a vessel myograph system (Danish Myotechnologies, Aarhus, Denmark). The aortas were bathed in oxygenated Krebs buffer and submitted to a resting tension of 9.8 mN. After 60 minutes of equilibration with frequent washings, concentration-response curves for phenylephrine (PE) were generated to determine vasoconstrictor responses. To study vasodilator and L-nitro arginine methyl ester (L-NAME) responses, the rings were preconstricted with a submaximal concentration of PE, and acetylcholine (ACh) (10^{-9} to 10^{-5} mol/L), sodium nitroprusside (SNP) (10^{-9} to 3×10^{-7} mol/L), or L-NAME (100 μmol/L) was injected at the plateau of the PE-induced contraction.

Atherosclerosis Model and Lesion Analysis

Apolipoprotein E-deficient (ApoE-KO) mice were purchased from The Jackson Laboratory (Bar Harbor, ME). ApoE-KO mice were bred with Trx2 TG mice to obtain ApoE-KO/Trx2-TG mice. Mice were genotyped by PCR with specific primers for ApoE and Trx2-TG transgene. Age-matched (6 to 8 weeks) and sex-matched WT, Trx2-TG, ApoE-KO, and ApoE-KO/Trx2-TG mice were fed normal chow (0.02% cholesterol, 4.5% total fat, 0% cholate) or atherogenic diet (1.25% cholesterol, 20% total fat, 0% cholate, catalog no. D12108; Research Diets, New Brunswick, NJ). Body weight was recorded, and blood samples were collected before and after diet. Total cholesterol, triglyceride, and high-density lipoprotein were determined by enzymatic assays (Sigma, St. Louis, MO). After 4 and 8 weeks of diet, mice were anesthetized by an intraperitoneal injection of 2,2,2-tribromoethanol (250 mg/kg), and the vascular tree was perfused with PBS under physiological pressure. Subsequently, the heart and aorta were removed, the arch and abdominal portions of the aorta were separated, and the heart and aortic arch were snap-frozen in OCT (Tissue-Tek, Torrance, CA).

To quantify the extent of atherosclerotic lesions, longitudinal sections of the aortic arch were analyzed microscopically in all mice after staining *en face* for lipids with Oil Red O. To quantify lipid deposition, frozen sections were fixed in 10% buffered formalin solution, rinsed in H_2O, and dehydrated in propylene glycol. Subsequently, slides were incubated in 0.5% Oil Red O solution in propylene glycol (60°C for 25 minutes), rinsed with H_2O, counterstained with hematoxylin, and coverslipped with glycerol gelatin. Aortic segments were also embedded in paraffin for routine immunohistochemistry with various antibodies: anti-CD31 (for ECs), Mac-3 (for macrophages), and anti-SMA (for smooth muscle cells) (BD Pharmingen, San Diego, CA) using NovaRed peroxidase substrate kit (Vector Laboratories, Burlingame, CA). All images were quantified by the NIH Image J Program (Bethesda, MD), and image analysis was performed independently by two investigators blinded to the genotype of the mice.

Results

EC-Specific Expression of Trx2

To determine the role of Trx2 in endothelium, we generated EC-specific transgenic mice by expressing the human Trx2 (with HA-tag at the C terminus) driven by an EC-specific VE-cadherin promoter[24] (Trx2 TG, Figure 1a). Eight founders (four males and four females) were obtained as determined by PCR genotyping (not shown) and Western blot of the tail tissues with anti-Trx2 antibody (Figure 1b). We chose two lines (lines 1 and 3, male) to backcross with C57BL/6 mice for more than six generations. All experiments were performed with heterozygous Trx2 TG mice and their non-TG littermates (WT) as controls. Trx2 mRNA from the two TG lines was highly expressed in the vascularized tissues including aorta, bone marrow, brain, heart, lung, and muscle as determined by qRT-PCR (Figure 1c). Trx2 protein in aortic tissue of Trx2 TG mice was fivefold higher than that in WT littermates as determined by Western blotting with anti-Trx2 antibody (Figure 1d). Furthermore, the Trx2 transgene was specifically detected in vascular endothelium as determined by immunohistochemistry (Figure 1e) or indirect immunofluorescence microscopy (Figure 1f) with anti-HA antibody that showed a co-staining with EC marker CD31 (Figure 1g). The Trx2 transgene was also detected in vasculature of other tissues (see Supplemental Figure S1, a and b, for heart and lung tissues at *http://ajp.amjpathol.org*). There were no apparent morphological abnormalities in Trx2 TG mice. Male and female mice seemed equally fertile, and there were no significant differences in grooming behavior, growth rate, or body weight (26.2 ± 6 g for Trx2 TG versus 25.3 ± 4.0 g for WT, $n = 20$), compared with WT littermates.

Trx2 TG Mice Show Increased Antioxidant Status, Reduced Oxidative Stress, Increased Serum NO Levels, and Reduced Blood Pressure

To determine the effects of Trx2 expression on vascular function in mouse, we determined total antioxidant status, oxidative stress, and NO levels in the serum from mice at the age of 3 to 4 months. Total antioxidant levels in Trx2 TG mice were nearly twofold higher than WT littermates (Figure 2a). 8-Isoprostane (a systemic oxidative marker in serum) in Trx2 TG was 2.5-fold lower than that in WT mice (Figure 2b). Serum NO levels (measured as NOx for both nitrite and nitrate) in Trx2 TG were significantly higher than WT littermates (Figure 2c). Because both Trx2 transgenic lines are similar in Trx2 expression, antioxidant status, and serum NO, we chose the Trx2 TG3 line for further studies. The reduced systemic oxidative stresses and increased plasma NO levels prompted us to determine blood pressure in Trx2 TG and WT mice. Heart rates were similar in anesthetized WT and Trx2 TG mice (Figure 2d); however, end diastolic, end systolic, and systemic blood pressure in Trx2 TG were significantly reduced (Figure 2, e–g, respectively). Infusion of nitric-oxide synthase (NOS) inhibitor L-NAME (100 μmol/L for 30 minutes)

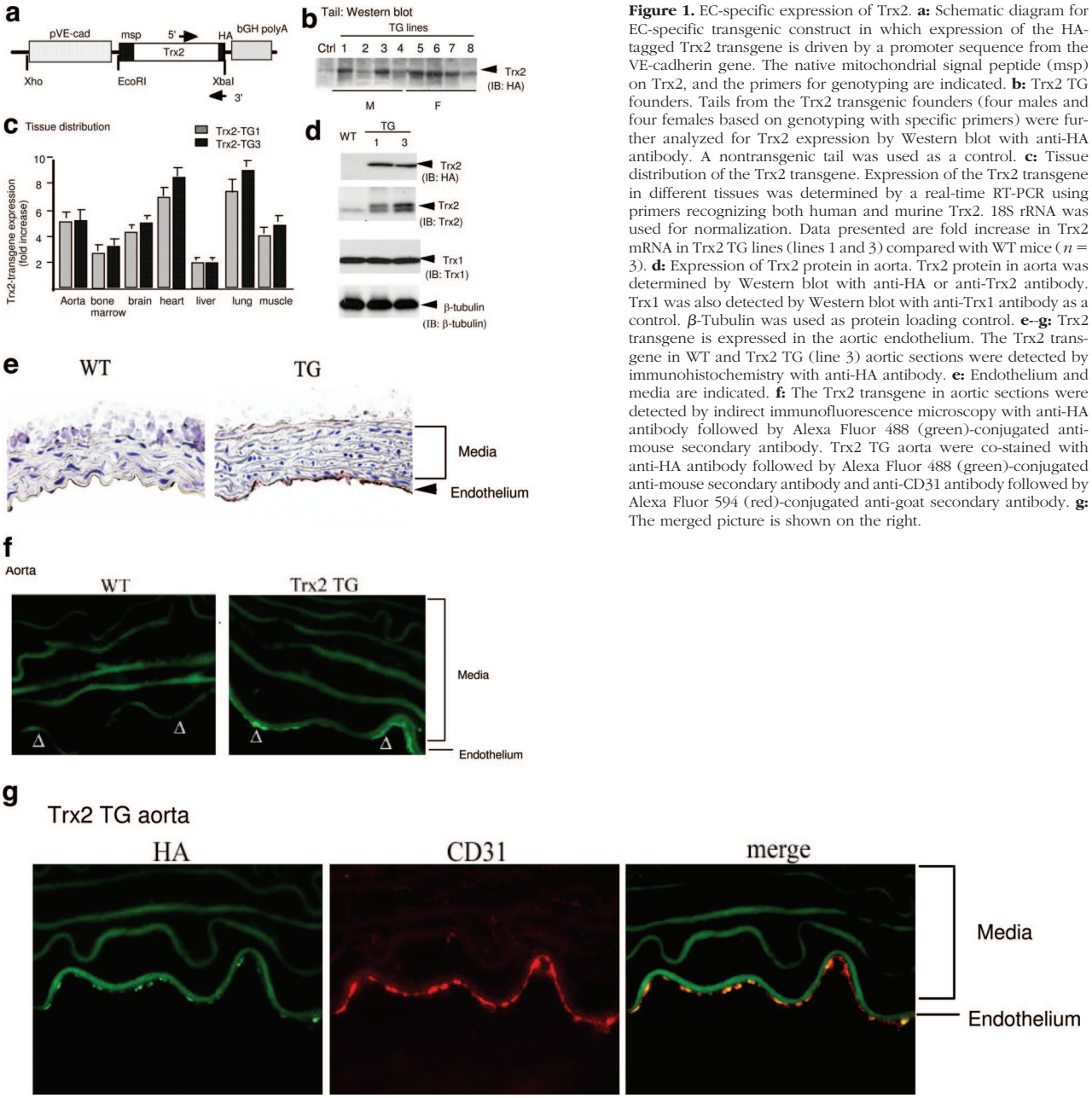

Figure 1. EC-specific expression of Trx2. **a:** Schematic diagram for EC-specific transgenic construct in which expression of the HA-tagged Trx2 transgene is driven by a promoter sequence from the VE-cadherin gene. The native mitochondrial signal peptide (msp) on Trx2, and the primers for genotyping are indicated. **b:** Trx2 TG founders. Tails from the Trx2 transgenic founders (four males and four females based on genotyping with specific primers) were further analyzed for Trx2 expression by Western blot with anti-HA antibody. A nontransgenic tail was used as a control. **c:** Tissue distribution of the Trx2 transgene. Expression of the Trx2 transgene in different tissues was determined by a real-time RT-PCR using primers recognizing both human and murine Trx2. 18S rRNA was used for normalization. Data presented are fold increase in Trx2 mRNA in Trx2 TG lines (lines 1 and 3) compared with WT mice (n = 3). **d:** Expression of Trx2 protein in aorta. Trx2 protein in aorta was determined by Western blot with anti-HA or anti-Trx2 antibody. Trx1 was also detected by Western blot with anti-Trx1 antibody as a control. β-Tubulin was used as protein loading control. **e**–**g:** Trx2 transgene is expressed in the aortic endothelium. The Trx2 transgene in WT and Trx2 TG (line 3) aortic sections were detected by immunohistochemistry with anti-HA antibody. **e:** Endothelium and media are indicated. **f:** The Trx2 transgene in aortic sections were detected by indirect immunofluorescence microscopy with anti-HA antibody followed by Alexa Fluor 488 (green)-conjugated anti-mouse secondary antibody. Trx2 TG aorta were co-stained with anti-HA antibody followed by Alexa Fluor 488 (green)-conjugated anti-mouse secondary antibody and anti-CD31 antibody followed by Alexa Fluor 594 (red)-conjugated anti-goat secondary antibody. **g:** The merged picture is shown on the right.

increased blood pressure in both WT and Trx2 TG mice to similar levels (Figure 2, e–g), suggesting that increased NO may contribute to the reduced blood pressures in Trx2 TG mice.

Trx2 TG Aortas Show Enhanced Endothelium-Dependent Relaxations

Increased serum NO levels in Trx2 TG mice prompted us to determine vascular reactivity of isolated aortic rings by examining the responses to the vasoconstrictor PE, endothelium-dependent vasodilator ACh and the NOS inhibitor L-NAME.[25] Aortas from Trx2 TG mice were less responsive to PE because 15-fold higher concentrations of PE were required to elicit constriction of the isolated aortic rings (EC_{50} = 2.0 ± 0.04 × 10^{-8} in WT versus 3.0 ± 0.05 × 10^{-7} in Trx2 TG (Figure 3a). To determine whether the basal release of eNOS-derived NO was different in WT versus TG vessels, aortic rings were preconstricted with a submaximal dose of PE, and the NOS inhibitor L-NAME (100 μmol/L) was added at the peak of the constriction to remove endogenous NO tone. L-NAME caused a further constriction in WT vessels, resulting in an increase in isometric tension reflecting the removal of basal NO. However, constriction of the vessel in response to L-NAME was much greater in aortas from Trx2 TG mice (Figure 3b). Figure 3c shows the ratio of EC_{50} by PE in the presence versus absence of L-NAME, and Trx2 TG vessel was sixfold greater than WT vessel. To determine the endothelium-dependent vasodilation of these

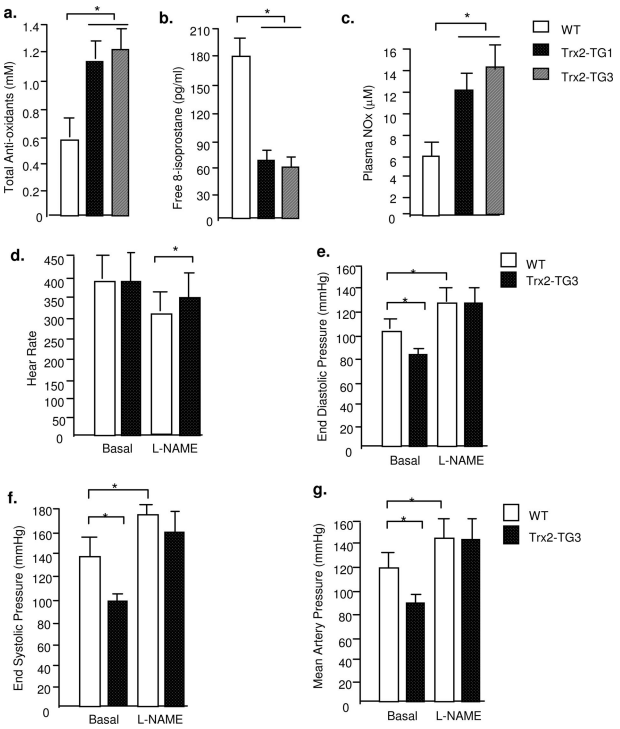

Figure 2. Hemodynamics in Trx2 TG mice. Serum from WT and Trx2 TG mice (both lines 1 and 3) were collected. **a:** Total antioxidant levels in the serum were measured by the Total Anti-Oxidant Status assay kit (Calbiochem) **b:** 8-Isoprostane, a systemic oxidative marker in serum, was determined by the enzyme-linked immunosorbent assay kit (Calbiochem). **c:** Serum NO was measured as NOx for both nitrite and nitrate (Cayman). **d:** Basal heart rate (minutes) was determined by echocardiography**. e–g:** End diastolic pressure, end systolic pressure, and mean artery pressure were determined at baseline and after administration of NO inhibitor L-NAME (0.1 mg/10 g body weight for 30 minutes). The number of mice in each group is shown in parentheses. $^*P < 0.05$, statistical significance between WT and Trx2 TG groups, $n = 9$ in each group.

vessels, ACh dose-response was examined. Aortas from Trx2 TG mice showed an enhanced response to ACh (Figure 3d). These effects on vasomotion occurred selectively in the endothelium because the vasoconstrictive responses to KCl and relaxation in response to the NO donor drug SNP were similar in the two strains (Figure 3, e and f). We conclude that vessels from Trx2 TG mice have an enhanced basal NO release and endothelium-dependent function.

Trx2 Increases NO Bioavailability in ECs by Scavenging Mitochondrial ROS

To further understand the mechanism by which Trx2 improves NO function, mouse ECs (MECs) were isolated from aortic tissues.[26] In isolated MECs, Trx2 expression was increased fivefold at the mRNA level and threefold at the protein level in Trx2 TG MECs (Figure 4a) and had no effect on the expression of endogenous components of the Trx2 antioxidant system (TrxR2 and Prx3) or other cellular ROS-scavenging enzymes (mitochondrial Mn-SOD, cytosolic catalase, and Trx1) (Figure 4, b and c). More importantly, the Trx2 transgene was localized in mitochondria as determined by cellular fractionation (Figure 4c) and was co-localized with cytochrome *c* in mitochondria (but not with Trx1 in the cytoplasm) as determined by confocal microscopy (see Supplemental Figure S2 at *http://ajp.amjpathol.org*). To measure NO release directly, MECs were stimulated with VEGF, and nitrite release into the culture media was measured by NO-specific chemiluminescence. Trx2 TG MECs showed fourfold higher basal levels of nitrite compared with WT MECs (Figure 4d). The increase in NO release from Trx2 TG MECs could be attributable to increased eNOS expression, phosphorylation, and/or enzymatic activity. To dissect these possibilities, eNOS phosphorylation on Ser1176 (an active form) was determined by Western blotting, and eNOS activity was also determined in lysates. No significant differences in the levels of total eNOS, phosphorylated eNOS (on Ser1179), or eNOS enzymatic activity were detected in the two cell types (Figure 4, e and f). These data suggest that Trx2 increases in NO bioactivity in ECs may regulate NO bioavailability without significant effects on eNOS regulation.

NO bioavailability can be regulated by intracellular ROS such as superoxide and hydrogen peroxide.[13,14] To determine whether Trx2 expression affects mitochondrial ROS generation, we determined mitochondrial ROS levels by flow cytometry analysis with dihydrorhodamine 123 (DHR123) and MitoTracker Red CM-H2XROS (MitoROS) probes, which preferentially detect mitochondrial ROS. TNF is a prototypic proinflammatory cytokine that primarily targets ECs, and it has been shown that TNF induces ROS generation in the mitochondria of ECs.[27,28] TNF induced ROS generation in ECs in a time-dependent manner, and ROS generation peaked at 2 hours (not shown). The basal mitochondrial ROS was reduced in Trx2 TG MECs compared with WT MECs as detected by DHR123 (Figure 5a, ctrl). Moreover, TNF-induced ROS was significantly blunted in Trx2 MECs as measured by DHR123 (Figure 5a, TNF) or MitoROS (Figure 5b). To determine directly whether Trx2 expression increases the scavenging of ROS, WT and Trx2 MECs were treated with paraquat (a reagent that induces cellular superoxide production) or H_2O_2 at 0.1 to 1 mmol/L, and mitochondrial ROS were measured with MitoROS and DHR123, respectively. Trx2 expression significantly enhanced EC capacity in scavenging paraquat-induced superoxide production (Figure 5c) and exogenous H_2O_2 (Figure 5d). These data suggest that Trx2 increases NO bioavailability in ECs by increasing EC capacity in scavenging mitochondrial ROS.

Endothelial Expression of Trx2 Prevents EC Dysfunction in ApoE-Deficient Mice

ApoE-deficient mice (ApoE) are a most widely used model for atherosclerosis. Aortas in these mice show increased oxidative mitochondrial damage and decreased endothelial function.[29–31] Accumulating evidence suggests that alterations in the NO pathway may play a central role in EC dysfunction induced by hypercholesterolemia. We hypothesize that loss of Trx2 function (decrease in expression or activity) during athero-

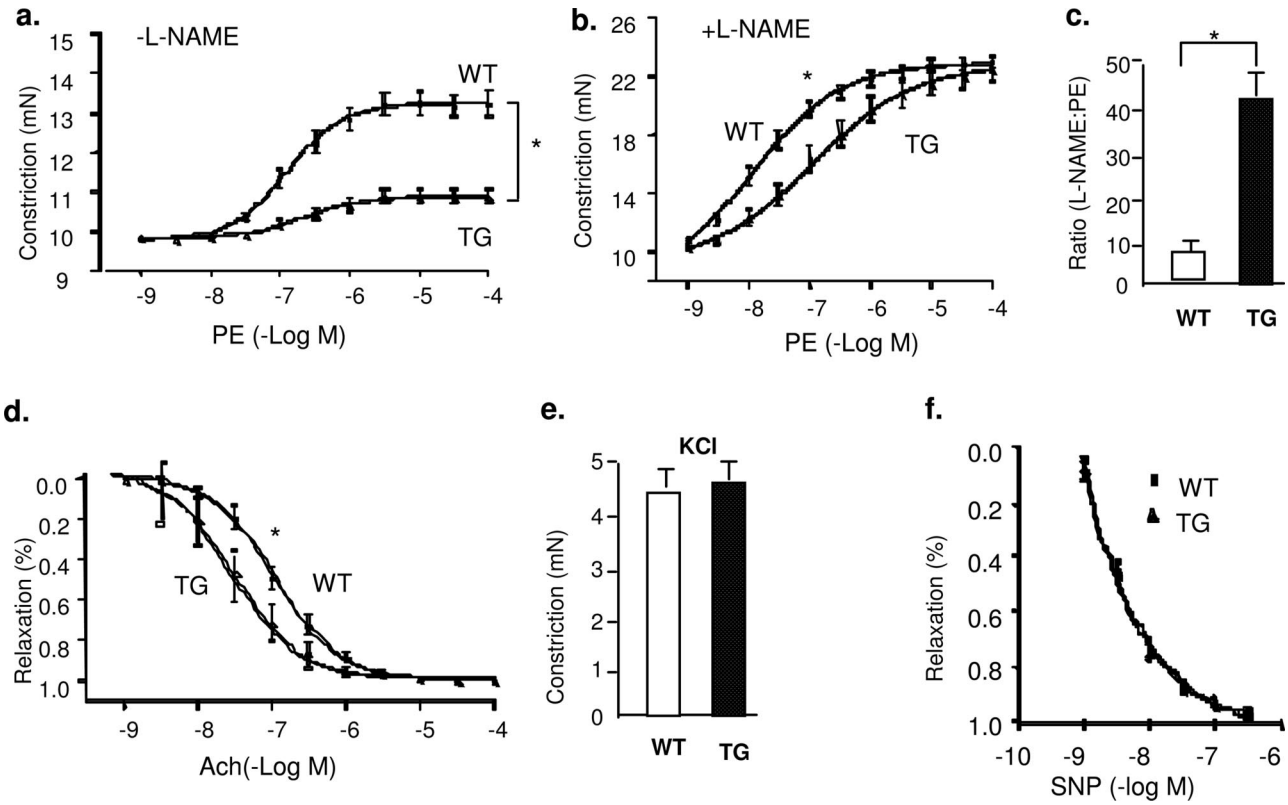

Figure 3. Trx2 transgene expression increases basal NO release in aortic endothelium. **a:** Aortas from Trx2 TG show an attenuated response to PE. Aortic rings were contracted with PE at a full range of doses (10^{-9} to 10^{-4} mol/L). Constriction force (mN) is shown. **b:** Basal NO is increased in Trx2 TG. Aortic rings were incubated with the NOS inhibitor L-NAME to remove basal NO synthesis and then contracted with PE as in **a**. **c:** Ratio of EC_{50} to PE in the presence versus absence of L-NAME (100 μmol/L). **d:** Aortas from Trx2 TG alter the response to ACh. Aortic rings were precontracted with PE and then relaxed with ACh at a full range of doses (10^{-9} to 10^{-4} mol/L). Percentage of relaxation is shown. **e:** Trx2 expression had no effects on vessel constriction in response to KCl. Aortic rings were contracted with 50 mmol/L KCl. **f:** Trx2 expression had no effects on vessel relaxation to the NO donor drug SNP. Aortic rings were incubated with a NOS inhibitor L-NAME to remove basal NO synthesis followed by a precontraction with PE as in **b** and were then relaxed with SNP at a full range of doses (10^{-9} to 10^{-6} mol/L). Data are presented are mean ± SEM, with $n = 5$ animals and eight aortic rings per animal. $^*P < 0.05$ indicates statistical significance by comparing WT versus TG at a dose, which causes 50% of constriction (PE) or relaxation (ACh).

sclerosis development/progression in ECs leads to an increase in ROS generation and that Trx2 transgene expression should reduce the development/progression of atherosclerosis. To test our hypothesis, we first characterized Trx2 expression in ApoE mice. Six- to 8-week-old C57BL/6 and ApoE mice were fed with normal chow or atherogenic diet for 4 weeks (for early lesions) or 8 weeks (for late lesions), and aortas were harvested for analysis. Lipid deposition in vessel wall determined by Oil Red O staining was detected in ApoE mice at 4 weeks but was dramatically increased at 8 weeks. Trx2 levels in aorta, particularly in the vascular endothelium, were dramatically reduced in ApoE mice compared with C57BL/6 mice immunohistochemistry and Western blot (see Supplemental Figure S3, a–c, at *http://ajp.amjpathol.org*). Trx1, phosphorylation of ASK1 (pThr-845, an active form induced by inflammatory and oxidative stress), and nitrotyrosine (an indicator of peroxynitrite-induced tyrosine nitrosylation) were determined by immunohistochemistry. Trx1 was not significantly altered in vasculature but seemed to be up-regulated in atherosclerotic plaques (see Supplemental Figure S3d at *http://ajp.amjpathol.org*), consisting with the previous reports.[32] Active ASK1 and oxidative/nitrosative stress marker nitrotyrosine were significantly increased in ApoE mice (see Supplemental Figure S3d at *http://ajp.amjpathol.org*).

EC dysfunction is an early event during atherosclerosis progression.[33,34] Thus, we determined vascular reactivity of aortic rings from ApoE mice at 4 weeks after diet. Vascular reactivity of aortic rings to the vasoconstrictor PE, to the endothelium-dependent vasodilator ACh, and to the eNOS inhibitor L-NAME was examined as we described previously.[25] Thoracic aorta from each mouse was cut into eight segments thus covering the entire aorta for the vascular reactivity measurements to eliminate variability attributable to lesions in different areas of the vessel. Consistent with previously results,[29–31] aortas from ApoE mice were less responsive to ACh but showed enhanced responses to PE (see Supplemental Figure S4 at *http://ajp.amjpathol.org*). To determine the effects of Trx2 on hypercholesterolemia-induced EC dysfunction, Trx2 TG were crossbred with ApoE-deficient mice to obtain ApoE-deficient/Trx2 TG mice (ApoE/TG). The mice were verified by genotyping and protein expression (not shown). The vascular reactivity between ApoE and ApoE/TG mice were compared as described for comparison between WT and Trx2 TG (Figure 3) and between WT and ApoE mice (see Supplemental Figure S3, a–c, at *http://ajp.amjpathol.org*). ApoE/TG showed re-

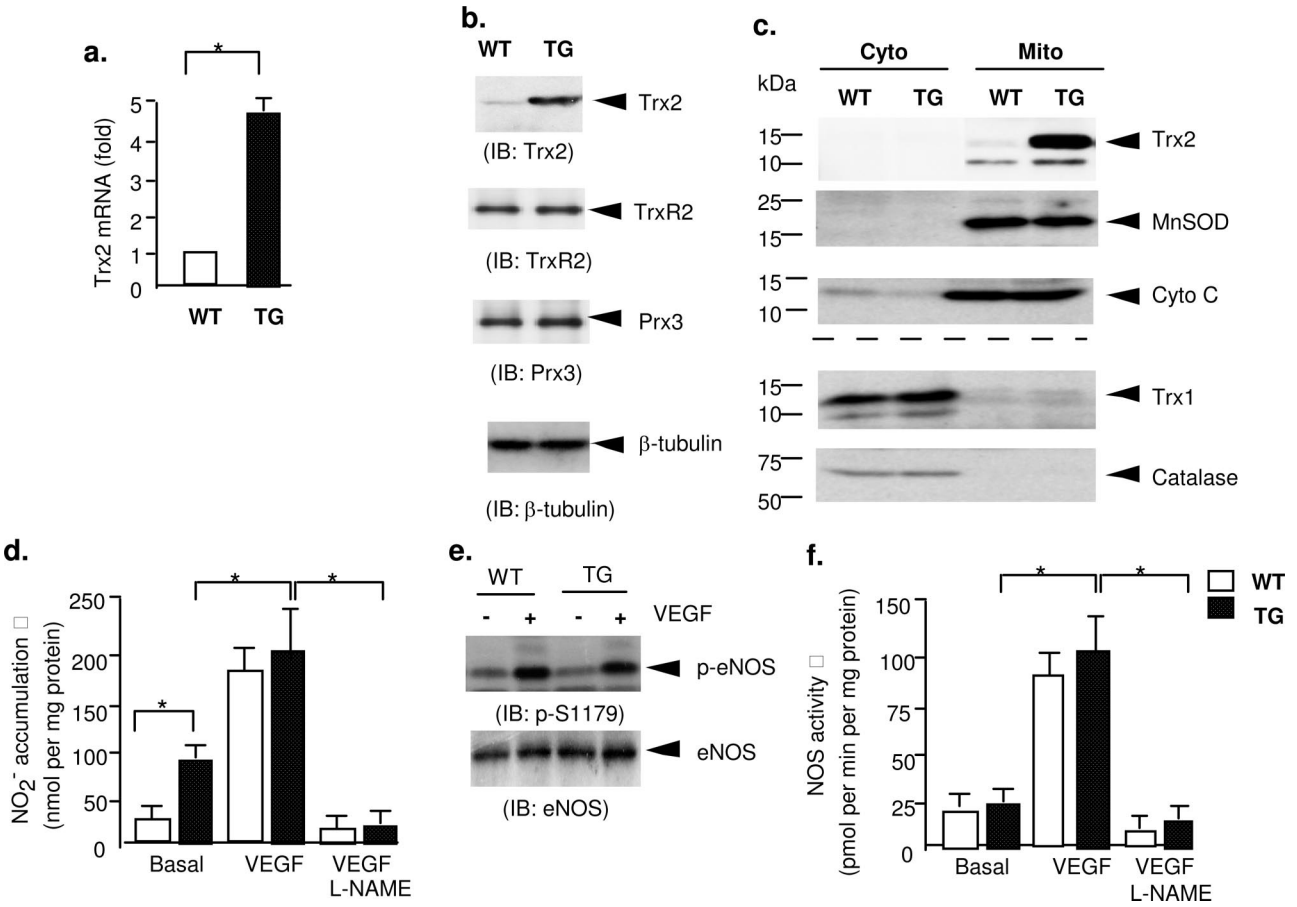

Figure 4. Trx2 increases NO bioavailability in ECs. Mouse aortic ECs (MECs) were isolated from WT and Trx2 TG mice. **a:** Trx2 mRNA was determined by qRT-PCR, and 18S rRNA was used for normalization. Data presented are fold increases in Trx2 MECs by taking WT MECs as 1.0. **b:** Trx2 expression had no effects on protein levels of TrxR2 or Prx3, components of the Trx2 antioxidant system. Trx2, TrxR2, and Prx3 proteins were determined by Western blot with anti-Trx2, anti-TrxR2, and anti-Prx3 antibody, respectively. β-Tubulin was used for protein normalization. **c:** Trx2 expression had no effects on protein levels or distributions of other ROS-scavenging enzymes. Cytoplasmic and mitochondrial fractions from WT and Trx2 TG MECs were isolated as described in Materials and Methods. Cytoplasmic and mitochondrial fractions were used for protein analyses. Cytosolic antioxidant enzymes (catalase and Trx1) and mitochondrial enzymes (Trx2 and MnSOD) were determined by Western blot with respective antibodies. Cytochrome *c* in mitochondria was used for protein normalization. **d–f:** Effects of Trx2 transgene on basal and VEGF-induced eNOS activity in MECs isolated from WT and Trx2 TG mice. MECs were cultured in media-deprived EC growth factors overnight followed by treatment with VEGF (50 ng/ml) in the absence or presence of eNOS inhibitor L-NAME (100 μmol/L) for 15 minutes (**d**) or 60 minutes (**e–f**). **d:** NO release was determined by measuring nitrite in the media. **e:** Phospho-(pSer1179) and total eNOS were determined by Western blot with respective antibodies. **f:** eNOS enzymatic activity was determined based on the conversion of [^{3}H]L-arginine to [^{3}H]L-citrulline according to the protocol from the manufacturer (Calbiochem). All eNOS activity and NO data presented are mean ± SEM of triplicates from three independent experiments. $^*P < 0.05$.

duced constriction in response to PE (Figure 6, a–d) but enhanced relaxation in response to ACh (Figure 6, e and f). These effects on vasomotion occurred selectively in the endothelium because the vasoconstrictive responses to KCl and relaxation in response to the NO donor drug SNP were similar in the two strains (Figure 6, g and h). More importantly, expression of Trx2 completely restored vascular reactivity from ApoE-deficient to WT phenotype (compare ApoE/TG in Figure 6 versus WT in Supplemental Figure S4). These results suggest that Trx2 expression in endothelium prevents hypercholesterolemia-induced NO reduction and EC dysfunction.

Trx2 Reduces Hypercholesterolemia-Induced Atherosclerotic Progression in ApoE-Deficient Mice

Finally, we determined the effects of Trx2 on atherosclerotic progression in ApoE mice. WT, Trx2 TG, ApoE, and ApoE/TG mice ($n = 10$) were fed with normal chow or atherogenic diet for 8 weeks. Chow- and atherogenic diet-fed ApoE mice showed increased levels of serum cholesterol compared with WT and TG mice. Trx2 had no significant effects on the basal and atherogenic diet-induced lipid levels (Figure 7a). In contrast, plasma NOx was significantly increased by Trx2 expression (Figure 7b). We then compared atherosclerotic lesion in the aortas of these mice using Oil Red O staining by analyzing the *en face* images (Figure 7c) or cross sections of the vessels (Figure 7e). Feeding an atherogenic diet significantly increased lesions in ApoE-deficient but not in WT or Trx2 TG mice (shown in Figure 7c for the diet groups, and quantified in Figure 7, d and f). Most importantly, ApoE/TG mice had significantly reduced lesions compared with ApoE mice. Thus, EC expression of Trx2 improves NO bioavailability by reducing ROS leading to a reduced progression of atherosclerotic lesions.

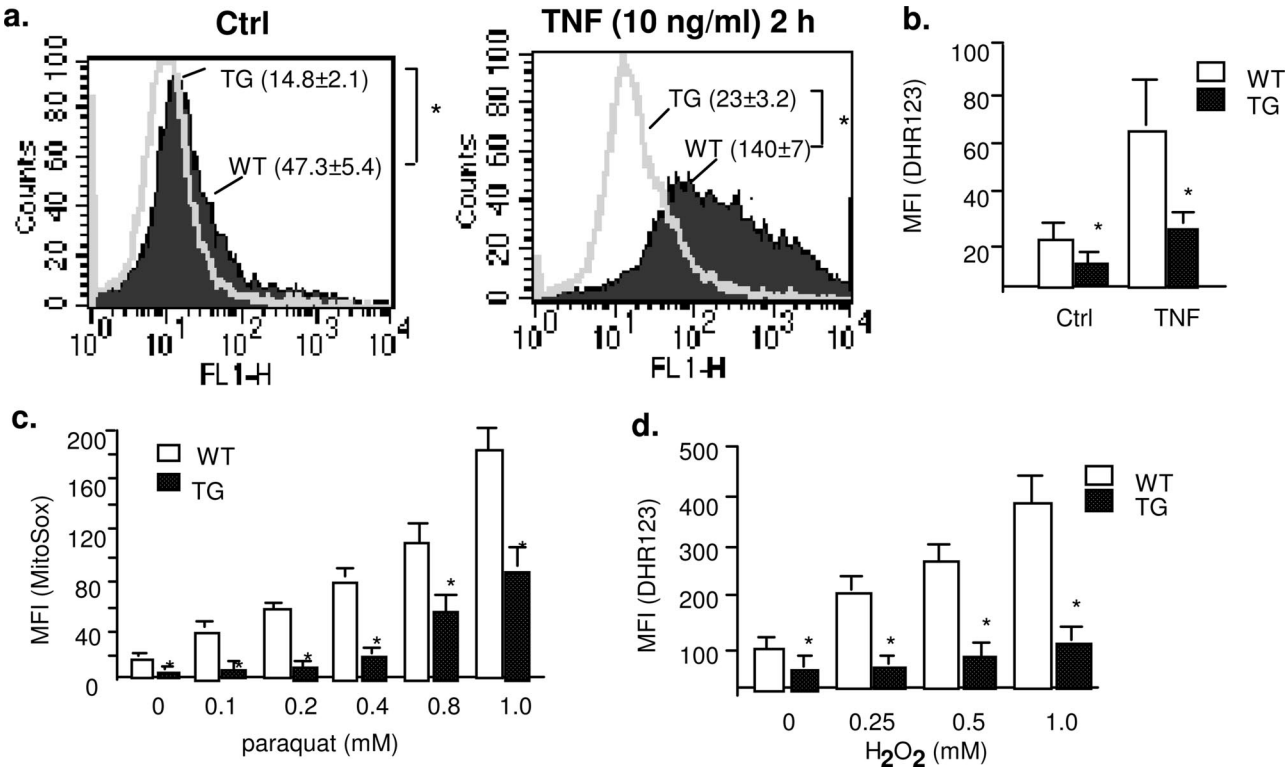

Figure 5. Trx2 increases EC capacity in scavenging ROS. **a** and **b:** Trx2 blocks TNF-induced mitochondrial ROS production. WT and Trx2 TG MECs were untreated or treated with TNF (10 ng/ml for 2 hours). Mitochondrial ROS was determined by flow cytometry with a specific probe DHR123 (**a**) or MitoTracker Red CM-H_2XROS (MitoROS) (**b**). Mean fluorescence intensity (MFI, mean ± SEM) from three independent experiments are indicated. **c:** Trx2 blocks paraquat-induced endogenous superoxide production in MECs. WT and Trx2 TG MECs were treated with paraquat overnight at indicated doses. **d:** Trx2 increases EC capacity in scavenging exogenous H_2O_2. MECs were treated with various concentrations of H_2O_2 (0 to 1 mmol/L for 30 minutes). Intracellular level of ROS was determined by flow cytometry analyses with DHR123 probe. Data presented are mean ± SEM from three independent experiments. $^*P < 0.05$.

Discussion

The knockout of Trx2 in mice resulted in embryonic lethality, and therefore the functions of the mitochondrial Trx2 system in the vasculature have not been investigated.[21] In the present study, by using EC-specific transgenesis of Trx2 gene in mice, we demonstrate a critical role of mitochondrial ROS and Trx2 in regulating various endothelial functions. Specifically, Trx2 TG mice have increased levels of total antioxidants in plasma and reduced systemic oxidative stress concomitant with an increase in NO levels and a decrease in blood pressure. Aortic rings from Trx2 TG mice show enhanced basal NO-dependent tone, which antagonizes the actions of the vasoconstrictor PE. Although total and phosphorylated (at pSer-1179) levels of eNOS as well as eNOS enzymatic activity are not increased in isolated ECs from Trx2 TG, NO bioavailability is dramatically increased in these cells. Moreover, Trx2 increases EC capacity to scavenge mitochondrial ROS, suggesting that Trx2 increases NO bioavailability by regulating intracellular ROS. More importantly, Trx2 improves EC function and reduces atherosclerotic lesions in the ApoE-deficient mice. Our data provide the first evidence that Trx2 plays a critical role in preserving vascular EC function and prevention of atherosclerosis development.

The mechanisms by which ROS regulates eNOS functions have been investigated.[13,14] In ECs, O_2^- generated from mitochondria not only alters endothelium-dependent vascular relaxation through interaction with NO, but the resultant nitrosative stress (N_2O_3 or peroxynitrite) can also oxidize eNOS cofactor BH_4. This causes a deficiency of BH4 and the putative uncoupling of eNOS leading to further increases in ROS generation.[13,14,35] H_2O_2 converted from O_2^- by MnSOD in mitochondria also contributes to the formation of nitrotyrosine by different pathways at the expense of NO in ECs. Furthermore, eNOS is regulated by *S*-nitrosylation, the covalent adduction of NO-derived nitrosyl groups to the cysteine thiols of proteins, resulting in reduction of eNOS enzymatic activity.[36,37] The effects of Trx2 on BH_4 levels, eNOS uncoupling, and eNOS nitrosylation need to be further examined.

The most important finding in our study is that Trx2 improves EC function and reduces atherosclerotic lesions in the ApoE-deficient mouse. Consistent with previous reports,[29–31] our data showed that endothelium-dependent relaxations in response to ACh are reduced whereas constrictions in response to PE are increased; these changes are attributable to reduction of NO bioavailability in the endothelium of ApoE-deficient mice. ApoE-deficient mice develop spontaneous hypercholesterolemia and aortic atherosclerosis. It has been shown that chemical inactivation of NO by ROS and reduced eNOS enzymatic activity are key mechanisms responsi-

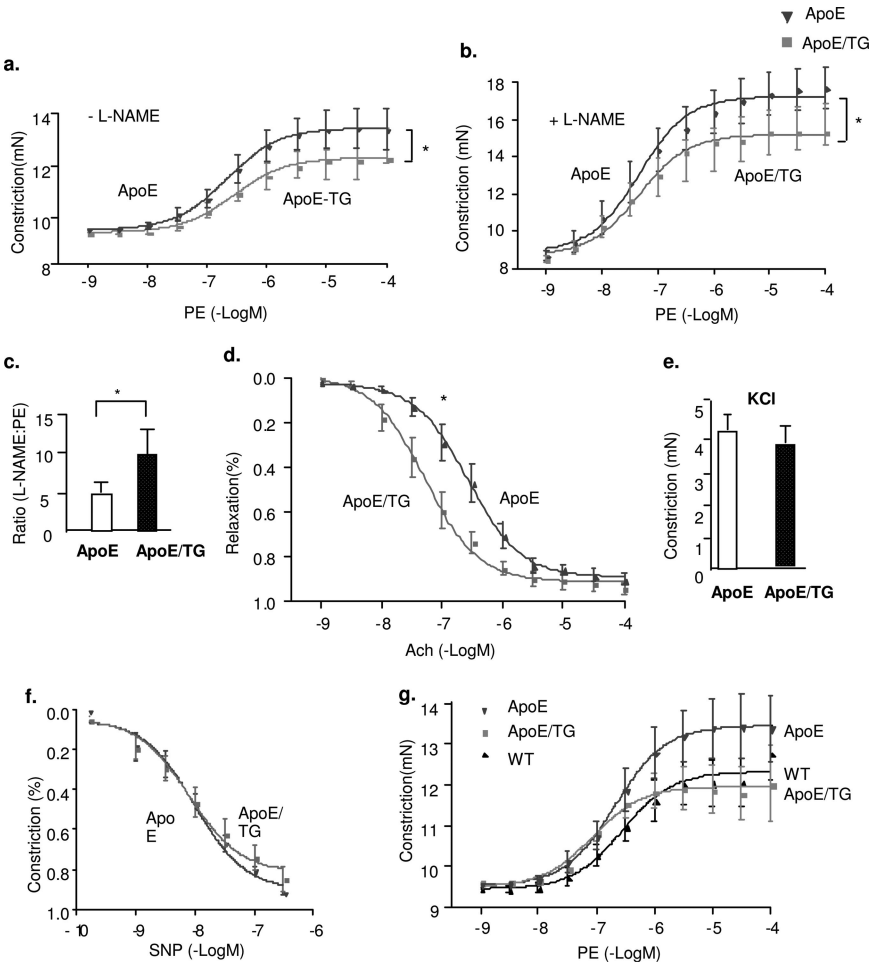

Figure 6. Trx2 prevents hypercholesterolemia-induced EC dysfunction in ApoE-deficient mice. WT, Trx2 TG, ApoE-deficient (ApoE), and ApoE-deficient/Trx2 TG mice (ApoE/TG) were fed with a Western-type diet for 4 weeks and vascular reactivity of aortic rings was determined as described in Figure 3. Only ApoE and ApoE/TG are shown in **a–e.** For comparison of WT and ApoE, see Supplemental Figure S4 at *http://ajp.amjpathol.org*. **a:** Aortic rings were contracted with PE at a full range of doses (10^{-9} to 10^{-4} mol/L). Constriction force (mN) is shown. **b:** Aortic rings were incubated with a NOS inhibitor L-NAME to remove basal NO synthesis and then contracted with PE as in **a**. **c:** Ratio of EC_{50} to PE in the presence versus absence of L-NAME (100 μmol/L). **d:** Aortic rings were contracted with ACh at a full range of doses (10^{-9} to 10^{-4} mol/L). Percentage of relaxation is shown. **e:** Aortic rings were contracted with 50 mmol/L of KCl. **f:** Aortic rings were incubated with a NOS inhibitor L-NAME to remove basal NO synthesis followed by a precontraction with PE as in **b** and were then relaxed with SNP at a full range of doses (10^{-9} to 10^{-6} mol/L). **g:** Comparison of the PE responses among WT, ApoE, and ApoE/TG. Aortic rings were contracted with PE at a full range of doses (10^{-9} to 10^{-4} mol/L). Constriction force is shown. All data are presented are mean ± SEM, with $n = 4$ animals and eight aortic rings per animal. $^*P <$ 0.05.

ble for endothelial dysfunction in aortas of atherosclerotic ApoE-deficient mice. Interestingly, we observed that Trx2 expression is decreased in ApoE-deficient aortas, indicating a potential mechanism by which hypercholesterol induces ROS generation. Thus, Trx2 transgene restores NO-dependent vascular function in aortas of atherosclerotic ApoE-deficient mice, suggesting that Trx2 transgene prevents hypercholesterol-induced reduction in NO bioavailability. Consistent with our genetic data, a similar study has been reported using a cell-permeable SOD mimetic that reduced superoxide production and partially normalized relaxations to ACh in ApoE-deficient mice.[29]

In the present study, the Trx2 transgene reduces atherosclerotic lesions in the ApoE-deficient mice. The role of ROS-generating or -scavenging enzymes in atherosclerosis progression has been previously investigated by using transgenic or genetically deficient mouse models. Mice overexpressing $p22^{phox}$, a subunit of NADPH oxidase generating ROS specifically in smooth muscle cells, had markedly increased atheroma formation in a carotid ligation model.[38] In contrast, overexpression of catalase or co-overexpression of catalase and Cu/Zn-SOD by transgene under their own promoters markedly retarded atherosclerosis in ApoE-KO mice.[39] Interestingly, overexpressing Cu/ZnSOD alone had no effect on atherosclerotic lesion formation.[39,40] Based on these studies, it has been speculated that H_2O_2 is more atherogenic than O_2^-.[14] Because the transgenes were expressed ubiquitously, the contributions of ROS-producing cell types such as vascular ECs, SMCs, and immune cells in the vessel wall have not been determined. To our best knowledge, the role of EC-derived ROS in atherogenesis has not been defined. Here, we show that Trx2 expression specifically in ECs dramatically enhances the capacity of ECs in scavenging both H_2O_2 and O_2^-, leading to improved EC function and reduced atherosclerosis, providing direct evidence for the critical role of EC-derived ROS in atherogenesis. The mechanism by which Trx2 scavenges ROS (both H_2O_2 and O_2^-) is not defined. Our data indicate that Trx2 expression had no effects on the level of MnSOD, catalase, TrxR2, or Prx3. It is conceivable that Trx2 may directly regulate scavenging ability of Prx3 or indirectly regulate mitochondrial redox state to maintain normal mitochondrial function, resulting in reduced ROS generation by mitochondria. On the other hand, Trx2 may indirectly regulate expression/activities of cytosolic antioxidant proteins. There has been recently demonstrated a crosstalk between mitochondria and NAD(P)H oxidase system in ROS production. Specifically, Desouki and colleagues[41] showed that mitochondria is critical for expression of NOX1, a member of nonphagocytic NAD(P)H oxidase proteins.[41,42] We are

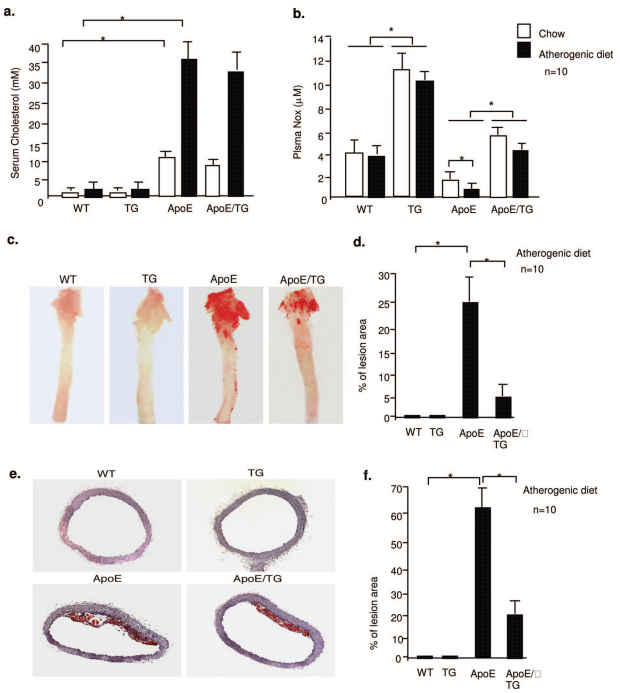

Figure 7. Trx2 reduces hypercholesterolemia-induced atherosclerotic progression in ApoE-deficient mice. WT, Trx2, ApoE-deficient (ApoE), and ApoE-deficient/Trx2 TG mice (ApoE/TG) ($n = 10$ for each group) were fed with a Western-type diet for 8 weeks. **a:** Serum cholesterol was measured enzymatically. **b:** Serum NO was measured as NOx for both nitrite and nitrate (Cayman). **c:** Whole aortas were harvested, opened longitudinally, and stained *en face* with Oil Red O. Percentage of lesion area was quantified in **d**. **e:** Paraffin sections from aortic arches (10 sections from each aorta) were stained with Oil Red O. Percentage of lesion area was quantified in **f**. Data are presented are mean ± SEM. $^*P < 0.05$.

investigating whether Trx2 overexpression alters the expression and/or activity of NAD(P)H oxidase proteins in ECs. Trx2 can also bind to and inhibit proapoptotic kinase ASK1.[23] Whether or not these activities of Trx2 are critical for its atheroprotective function is currently under investigation. Nevertheless, our data highlight the critical role of the mitochondrial Trx2 system in endothelial redox biology and in the prevention of atherosclerosis.

Acknowledgment

We thank Dr. Laura Benjamin for VE-cadherin promoter constructs.

References

1. Ballinger SW, Patterson C, Knight-Lozano CA, Burow DL, Conklin CA, Hu Z, Reuf J, Horaist C, Lebovitz R, Hunter GC, McIntyre K, Runge MS: Mitochondrial integrity and function in atherogenesis. Circulation 2002, 106:544–549
2. Nishikawa T, Edelstein D, Du XL, Yamagishi S, Matsumura T, Kaneda Y, Yorek MA, Beebe D, Oates PJ, Hammes HP, Giardino I, Brownlee M: Normalizing mitochondrial superoxide production blocks three pathways of hyperglycaemic damage. Nature 2000, 404:787–790
3. Wolin MS: Interactions of oxidants with vascular signaling systems. Arterioscler Thromb Vasc Biol 2000, 20:1430–1442
4. Cai H: NAD(P)H oxidase-dependent self-propagation of hydrogen peroxide and vascular disease. Circ Res 2005, 96:818–822
5. Ignarro LJ, Napoli C, Loscalzo J: Nitric oxide donors and cardiovascular agents modulating the bioactivity of nitric oxide: an overview. Circ Res 2002, 90:21–28
6. Bath PM: The effect of nitric oxide-donating vasodilators on monocyte chemotaxis and intracellular cGMP concentrations in vitro. Eur J Clin Pharmacol 1993, 45:53–58
7. Lefer AM, Ma XL: Decreased basal nitric oxide release in hypercholesterolemia increases neutrophil adherence to rabbit coronary artery endothelium. Arterioscler Thromb 1993, 13:771–776
8. Keaney Jr JF: Oxidative stress and the vascular wall: NADPH oxidases take center stage. Circulation 2005, 112:2585–2588
9. Hansen JM, Go YM, Jones DP: Nuclear and mitochondrial compartmentation of oxidative stress and redox signaling. Annu Rev Pharmacol Toxicol 2006, 46:215–234
10. Schriner SE, Linford NJ, Martin GM, Treuting P, Ogburn CE, Emond M, Coskun PE, Ladiges W, Wolf N, Van Remmen H, Wallace DC, Rabinovitch PS: Extension of murine life span by overexpression of catalase targeted to mitochondria. Science 2005, 308:1909–1911
11. Ramachandran A, Levonen AL, Brookes PS, Ceaser E, Shiva S, Barone MC, Darley-Usmar V: Mitochondria, nitric oxide, and cardiovascular dysfunction. Free Radic Biol Med 2002, 33:1465–1474
12. Balaban RS, Nemoto S, Finkel T: Mitochondria, oxidants, and aging. Cell 2005, 120:483–495
13. Landmesser U, Dikalov S, Price SR, McCann L, Fukai T, Holland SM, Mitch WE, Harrison DG: Oxidation of tetrahydrobiopterin leads to uncoupling of endothelial cell nitric oxide synthase in hypertension. J Clin Invest 2003, 111:1201–1209
14. Cai H: Hydrogen peroxide regulation of endothelial function: origins, mechanisms, and consequences. Cardiovasc Res 2005, 68:26–36
15. Drummond GR, Cai H, Davis ME, Ramasamy S, Harrison DG: Transcriptional and posttranscriptional regulation of endothelial nitric oxide synthase expression by hydrogen peroxide. Circ Res 2000, 86:347–354
16. Rhee SG: Redox signaling: hydrogen peroxide as intracellular messenger. Exp Mol Med 1999, 31:53–59
17. Connor KM, Subbaram S, Regan KJ, Nelson KK, Mazurkiewicz JE, Bartholomew PJ, Aplin AE, Tai YT, Aguirre-Ghiso J, Flores SC, Melendez JA: Mitochondrial H2O2 regulates the angiogenic phenotype via PTEN oxidation. J Biol Chem 2005, 280:16916–16924
18. Spyrou G, Enmark E, Miranda-Vizuete A, Gustafsson J: Cloning and expression of a novel mammalian thioredoxin. J Biol Chem 1997, 272:2936–2941
19. Holmgren A: Antioxidant function of thioredoxin and glutaredoxin systems. Antioxid Redox Signal 2000, 2:811–820
20. Chang TS, Cho CS, Park S, Yu S, Kang SW, Rhee SG: Peroxiredoxin III, a mitochondrion-specific peroxidase, regulates apoptotic signaling by mitochondria. J Biol Chem 2004, 279:41975–41984
21. Tanaka T, Hosoi F, Yamaguchi-Iwai Y, Nakamura H, Masutani H, Ueda S, Nishiyama A, Takeda S, Wada H, Spyrou G, Yodoi J: Thioredoxin-2 (TRX-2) is an essential gene regulating mitochondria-dependent apoptosis. EMBO J 2002, 21:1695–1703
22. Fulton D, Gratton JP, McCabe TJ, Fontana J, Fujio Y, Walsh K, Franke TF, Papapetropoulos A, Sessa WC: Regulation of endothelium-derived nitric oxide production by the protein kinase Akt. Nature 1999, 399:597–601
23. Zhang R, Al-Lamki R, Bai L, Streb JW, Miano JM, Bradley J, Min W: Thioredoxin-2 inhibits mitochondria-located ASK1-mediated apoptosis in a JNK-independent manner. Circ Res 2004, 94:1483–1491
24. Sun JF, Phung T, Shiojima I, Felske T, Upalakalin JN, Feng D, Kornaga T, Dor T, Dvorak AM, Walsh K, Benjamin LE: Microvascular patterning is controlled by fine-tuning the Akt signal. Proc Natl Acad Sci USA 2005, 102:128–133
25. Bauer PM, Yu J, Chen Y, Hickey R, Bernatchez PN, Looft-Wilson R, Huang Y, Giordano F, Stan RV, Sessa WC: Endothelial-specific expression of caveolin-1 impairs microvascular permeability and angiogenesis. Proc Natl Acad Sci USA 2005, 102:204–209
26. Ackah E, Yu J, Zoellner S, Iwakiri Y, Skurk C, Shibata R, Ouchi N, Easton RM, Galasso G, Birnbaum MJ, Walsh K, Sessa WC: Akt1/protein kinase Balpha is critical for ischemic and VEGF-mediated angiogenesis. J Clin Invest 2005, 115:2119–2127
27. Corda S, Laplace C, Vicaut E, Duranteau J: Rapid reactive oxygen species production by mitochondria in endothelial cells exposed to tumor necrosis factor-alpha is mediated by ceramide. Am J Respir Cell Mol Biol 2001, 24:762–768

28. Deshpande SS, Angkeow P, Huang J, Ozaki M, Irani K: Rac1 inhibits TNF-alpha-induced endothelial cell apoptosis: dual regulation by reactive oxygen species. FASEB J 2000, 14:1705–1714
29. d'Uscio LV, Baker TA, Mantilla CB, Smith L, Weiler D, Sieck GC, Katusic ZS: Mechanism of endothelial dysfunction in apolipoprotein E-deficient mice. Arterioscler Thromb Vasc Biol 2001, 21:1017–1022
30. Ohara Y, Peterson TE, Harrison DG: Hypercholesterolemia increases endothelial superoxide anion production. J Clin Invest 1993, 91:2546–2551
31. Stroes E, Kastelein J, Cosentino F, Erkelens W, Wever R, Koomans H, Luscher T, Rabelink T: Tetrahydrobiopterin restores endothelial function in hypercholesterolemia. J Clin Invest 1997, 99:41–46
32. Okuda M, Inoue N, Azumi H, Seno T, Sumi Y, Hirata K, Kawashima S, Hayashi Y, Itoh H, Yodoi J, Yokoyama M: Expression of glutaredoxin in human coronary arteries: its potential role in antioxidant protection against atherosclerosis. Arterioscler Thromb Vasc Biol 2001, 21:1483–1487
33. Ross R: Atherosclerosis—an inflammatory disease. N Engl J Med 1999, 340:115–126
34. Libby P: Inflammation in atherosclerosis. Nature 2002, 420:868–874
35. Stocker R, Keaney Jr JF: Role of oxidative modifications in atherosclerosis. Physiol Rev 2004, 84:1381–1478
36. Erwin PA, Lin AJ, Golan DE, Michel T: Receptor-regulated dynamic S-nitrosylation of endothelial nitric-oxide synthase in vascular endothelial cells. J Biol Chem 2005, 280:19888–19894
37. Ravi K, Brennan LA, Levic S, Ross PA, Black SM: S-nitrosylation of endothelial nitric oxide synthase is associated with monomerization and decreased enzyme activity. Proc Natl Acad Sci USA 2004, 101:2619–2624
38. Khatri JJ, Johnson C, Magid R, Lessner SM, Laude KM, Dikalov SI, Harrison DG, Sung HJ, Rong Y, Galis ZS: Vascular oxidant stress enhances progression and angiogenesis of experimental atheroma. Circulation 2004, 109:520–525
39. Yang H, Roberts LJ, Shi MJ, Zhou LC, Ballard BR, Richardson A, Guo ZM: Retardation of atherosclerosis by overexpression of catalase or both Cu/Zn-superoxide dismutase and catalase in mice lacking apolipoprotein E. Circ Res 2004, 95:1075–1081
40. Tribble DL, Gong EL, Leeuwenburgh C, Heinecke JW, Carlson EL, Verstuyft JG, Epstein CJ: Fatty streak formation in fat-fed mice expressing human copper-zinc superoxide dismutase. Arterioscler Thromb Vasc Biol 1997, 17:1734–1740
41. Desouki MM, Kulawiec M, Bansal S, Das GM, Singh KK: Cross talk between mitochondria and superoxide generating NADPH oxidase in breast and ovarian tumors. Cancer Biol Ther 2005, 4:1367–1373
42. Gutierrez J, Ballinger SW, Darley-Usmar VM, Landar A: Free radicals, mitochondria, and oxidized lipids: the emerging role in signal transduction in vascular cells. Circ Res 2006, 99:924–932